



Hamilton, H., King, A., Sparkes, H., Pridmore, N., & Wass, D. (2019). Zirconium-Nitrogen Intermolecular Frustrated Lewis Pairs. *Inorganic Chemistry*, 58(9), 6399-6409.
<https://doi.org/10.1021/acs.inorgchem.9b00569>

Peer reviewed version

Link to published version (if available):
[10.1021/acs.inorgchem.9b00569](https://doi.org/10.1021/acs.inorgchem.9b00569)

[Link to publication record in Explore Bristol Research](#)
PDF-document

This is the author accepted manuscript (AAM). The final published version (version of record) is available online via ACS at <https://pubs.acs.org/doi/10.1021/acs.inorgchem.9b00569> . Please refer to any applicable terms of use of the publisher.

University of Bristol - Explore Bristol Research

General rights

This document is made available in accordance with publisher policies. Please cite only the published version using the reference above. Full terms of use are available:
<http://www.bristol.ac.uk/red/research-policy/pure/user-guides/ebr-terms/>

Zirconium-Nitrogen Intermolecular Frustrated Lewis Pairs

Hugh B. Hamilton,[†] Ashley M. King,[†] Hazel A. Sparkes,[†] Natalie E. Pridmore,[†] Duncan F. Wass^{,‡}*

[†]School of Chemistry, University of Bristol, Cantock's Close, Bristol, BS8 1TS, United Kingdom

[‡]School of Chemistry, Cardiff University, Main Building, Park Place, Cardiff, CF10 3AT, United Kingdom

ABSTRACT

A series of intermolecular transition metal frustrated Lewis pairs (FLPs) based on zirconocene and nitrogen Lewis base moieties have been reported and reacted with D₂, CO₂, THF, PhCCD. The catalytic dehydrocoupling of Me₂NH·BH₃ is also reported. Comparisons can be made with previous work employing phosphines, and greater insight into the importance of both steric and electronic effects of the Lewis base have been gleaned as a result. Exploration of the role hard-hard or hard-soft acid-base interactions may play seems to suggest that these effects take a back-seat to the more prominent roles of steric bulk and basicity.

INTRODUCTION

Frustrated Lewis pairs (FLPs) first came to prominence over a decade ago,¹ and the subject area is continuing to reveal powerful new chemistry for small molecule activation and catalysis. Main group FLPs have been the focus of much of this chemistry, having been used to perform a wide variety of transformations with both *inter*- and *intra*-molecular systems.^{2, 3}

We have focused on the use of Zr(IV) cations as the Lewis acidic component in FLPs, which have predominantly taken the form of a zirconocene in combination with an intramolecular phosphine moiety; other groups have taken a similar approach (Figure 1). The FLPs produced (**A-H**) have been used for the effective activation of a number of small molecules including H₂, CO₂, H₂CO, PhCCH, C₂H₄, THF, Et₂O, Me₂CO, in addition to performing the cleavage of C-Cl and C-F bonds, and catalytic amine-borane dehydrocoupling.⁴⁻¹¹

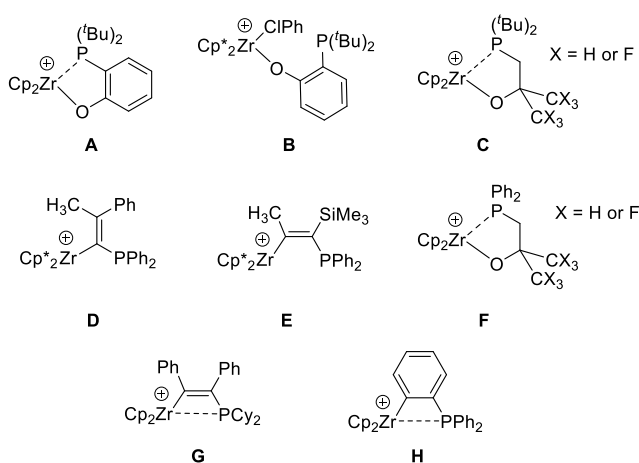
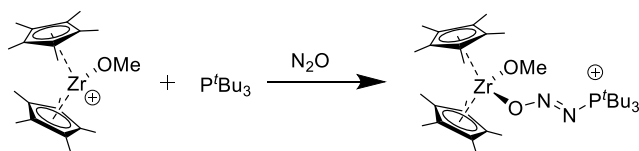


Figure 1. Intramolecular Zr/P FLPs developed by our group (**A-C**) and by Erker *et al.* (**D-H**). In all cases, the [B(C₆F₅)₄][−] or [MeB(C₆F₅)₃][−] counterion has been omitted for clarity.

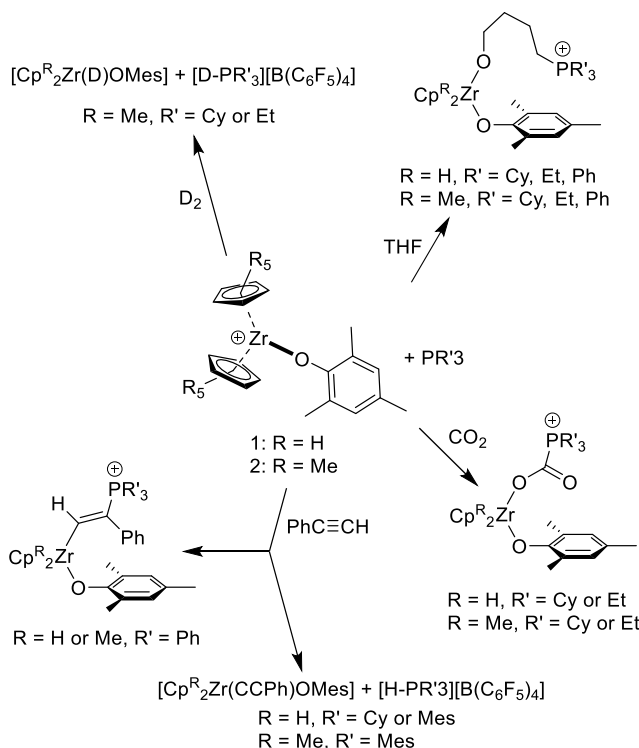
Intermolecular main group FLPs have been explored in parallel with intramolecular examples;² by contrast, intermolecular transition metal FLPs are far less explored with only the activation of N₂O using a Zr(IV)/P^tBu₃ FLP reported by Stephan *et al.* (Scheme 1),¹² and a wider exploration of intermolecular Zr(IV)/phosphine systems reported by our group in 2016 (Scheme 2).^{13, 14} The

activation of CO₂ and H₂, along with the ring-opening of THF and activation of phenylacetylene (via both proton abstraction and 1,2-addition), by this latter system shows that these more easily modified (and less synthetically challenging) systems can achieve the same useful chemistry.

Scheme 1. Intermolecular Zr/P FLP used for N₂O activation



Scheme 2. Intermolecular Zr/P FLPs developed by our group. [B(C₆F₅)₄][−] counterion omitted for clarity



An outstanding question for Zr(IV)-based FLPs is the extent to which the hard-soft mismatch between the hard zirconocene centre and the soft phosphine Lewis base influences the ‘frustration’ of the FLP produced. Do Zr(IV)-amine pairs, in which a stronger hard-hard interaction is expected, still behave as FLPs? Amines have already been widely used in main group FLP chemistry.¹⁵⁻³⁰

An intramolecular example (**M**, Figure 2) has been reported and was able to perform H₂ activation, chloride abstraction from CH₂Cl₂, and proton abstraction from phenylacetylene – all well-established FLP reactions.⁹ We have also reported that Zr(IV) cations catalyze the hydrogenation of imines, whereby the imine itself acts as the Lewis basic component of an FLP.³¹

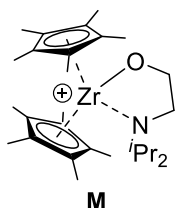


Figure 2. Zr/N FLP **M** developed by Erker *et al.* [B(C₆F₅)₄][−] counterion omitted for clarity.

This paper demonstrates that pairs formed from zirconocenes with a wider variety of amine bases and effective and versatile FLPs.

RESULTS AND DISCUSSION

Previously, the Zr(IV) cations **1** and **2** (Figure 3) were combined with a series of phosphines in order to perform FLP-type reactions;¹³ the same Zr(IV) cations were explored in a similar way with a group of nitrogen-based Lewis bases. The selection of nitrogen compounds was chosen due to the varying basicities and steric bulk of the different species, with NEt₃ (**a**, pK_a = 10.8) and ⁱPr₂NEt (**b**, pK_a = 11.4) being more basic than pyridine (**c**, pK_a = 5.3) and its derivatives 2-methylpyridine (**d**, pK_a = 5.9) and 2,6-dimethylpyridine (**e**, pK_a = 6.8).³²⁻³⁵

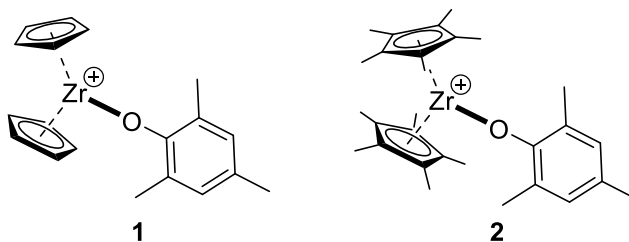


Figure 3. The Zr(IV) cations used in this work. The [B(C₆F₅)₄][−] counterions has been omitted for clarity.

When **1** is mixed with **a-e**, a lightening of the yellow solution is seen in all cases upon addition of the Lewis base. The reaction of **2** with **a**, **b** and **e** resulted in a color change from orange to deep red, whereas the addition of **c** and **d** gave green and lighter orange solutions respectively. Examining these interactions by ^{15}N NMR spectroscopy gave inconclusive results. However, by using ^{15}N -HMBC NMR spectroscopy reliable data was obtained; the results and comparison to the free Lewis base resonances are shown in Table 1. The correlating data for **1c** was unobtainable due to a very weak signal, and **2b** resulted in FLP degradation and formation of $[\text{H-N}(\textit{i}\text{Pr})_2\text{Et}][\text{B}(\text{C}_6\text{F}_5)_4]$ within the timeframe of the experiment. Comparing, for example, free NEt_3 (**a**) with **1a** and **1b**, it is apparent from the large change in chemical shift that a strong Lewis pair interaction results with the less bulky zirconocene **1** whereas only a small shift is observed for the bulky **2**. For less basic pyridine-type bases results are more inconclusive with the suggestion of a weaker interaction.

Table 1. ^{15}N -HMBC NMR chemical shifts of the Lewis bases **a-e** and the Lewis pairs **1a-e** and **2a-e**

| Lewis base | ^{15}N - HMBC NMR, δ/ppm | Zr/N | ^{15}N - HMBC NMR, δ/ppm | Zr/N | ^{15}N - HMBC NMR, δ/ppm |
|---|--|-----------|--|-----------|--|
| NEt_3 (a) | 47.6 | 1a | 163.5 | 2a | 54.2 |
| $\textit{i}\text{Pr}_2\text{NEt}$ (b) | 57.5 | 1b | 185.5 | 2b | - |
| $\text{C}_5\text{H}_5\text{N}$ (c) | 318.9 | 1c | - | 2c | 260.5 |
| $\text{C}_5\text{H}_4(\text{CH}_3)\text{N}$ (d) | 317.7 | 1d | 302.1 | 2d | 261.1 |
| $\text{C}_5\text{H}_3(\text{CH}_3)_2\text{N}$ (e) | 317.2 | 1e | 249.8 | 2e | 286.0 |

DOSY (Diffusion-Ordered SpectroscopY) NMR spectroscopy has proved to be a useful tool in FLP chemistry, the interaction between the Lewis acid and Lewis base being dynamic in nature,

with an equilibrium between the “bound” and “unbound” states. The degree to which the equilibrium lies towards either state depends upon the specific Lewis pair, and the relative diffusion coefficients (D) of the separate components and pair are revealing. This analysis proved useful with our previous Zr/P systems,¹³ indicating that some ‘frustration’ is present even if the equilibrium lies well towards the bound pair; this was born out in the reactivity pattern observed. The diffusion coefficients (D) of the free and combined species can be seen in Table 2.

Table 2. The diffusion coefficients (D) of the free and combined Lewis pair species, with all results obtained using PhBr- d_5 at a concentration of 0.06 mol dm⁻³. All values have units of $\times 10^{-10}$ m² s⁻¹.
¹. D of **1** in absence of base is 6.0×10^{-10} m² s⁻¹. D of **2** in absence of base is 8.6×10^{-10} m² s⁻¹.

| Lewis Base | D of base | D of base with 1 | D of base with 2 | D of 1 with base | D of 2 with base |
|--|-------------------|------------------------------------|------------------------------------|------------------------------------|------------------------------------|
| NEt ₃ (a) | 9.2 | 8.2 | 8.7 | 3.3 | 4.4 |
| ^{<i>i</i>} Pr ₂ NEt (b) | 8.6 | 9.0 | 9.0 | 3.3 | 3.6 |
| C ₅ H ₅ N (c) | 11.8 | 5.7 | 4.0 | 3.3 | 3.3 |
| C ₅ H ₄ (CH ₃)N (d) | 11.0 | 5.2 | 5.2 | 2.5 | 2.3 |
| C ₅ H ₃ (CH ₃) ₂ N (e) | 9.7 | 6.8 | 6.8 | 2.3 | 2.1 |

The results are somewhat surprising in that **a** and **b** have similar diffusion coefficients in the presence or absence of either zirconocene, suggesting pair-separated species predominate even though these aliphatic amines are the most basic. By contrast, pyridine-derived bases **c-e** have significantly smaller diffusion coefficients in the presence of **1** or **2**, suggesting a more persistent interaction. A possible explanation is the more planar geometry of **c-e** facilitating a minimization of steric clash in comparison to the more 3-dimensional **a** and **b**. It is also noteworthy that **1** and **2**, despite significant steric differences, show similar results. This is in contrast to similar

experiments with phosphine bases where the less sterically encumbered **1** showed a marked tendency to form less dynamic pairs.

Single crystals of **2c** and **2d** suitable for X-ray diffraction study were obtained and the solid-state structures of **2c** and **2d** are shown in Figure 4. **2c** possesses a shorter Zr—N bond (2.326(3) Å) than **2d** (2.386(4) Å), likely a result of the increased steric bulk of **d**. Complex **2c** also has greater bending of the alkoxide fragment (bond angle Zr1—O1—C26 158.8(2)°) compared to **2d** (Zr1—O1—C21 167.4(3)°); in **2**, this angle is almost completely linear (176.7(2)°). Whilst it is tempting to rationalize this effect in terms of the multiple bond character between the Zr and O atoms changing according to other donor ligands, alkoxide bond angles are known to be an unreliable indicator of such effects and a steric rationale is also possible.¹³

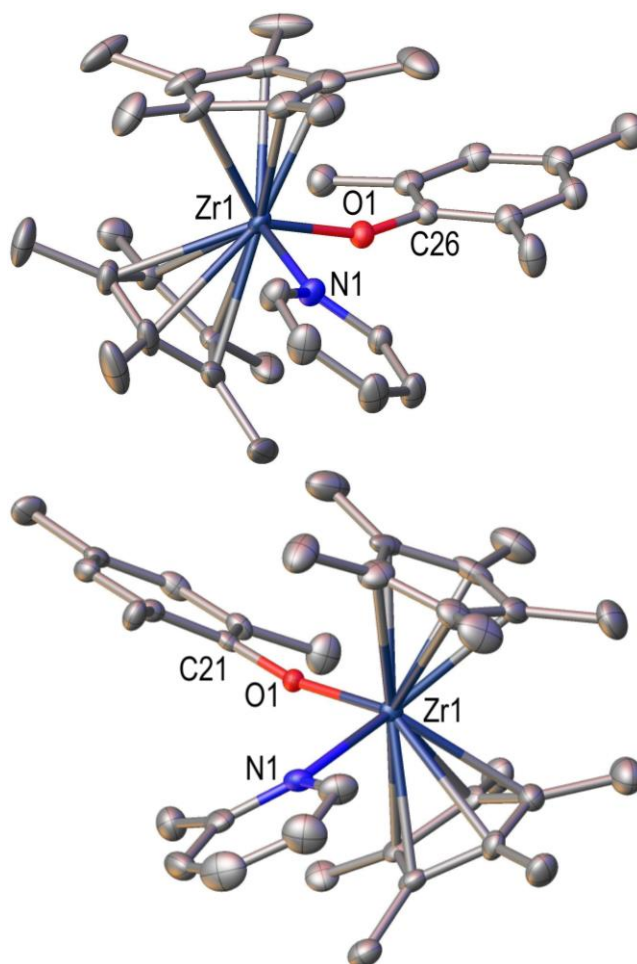


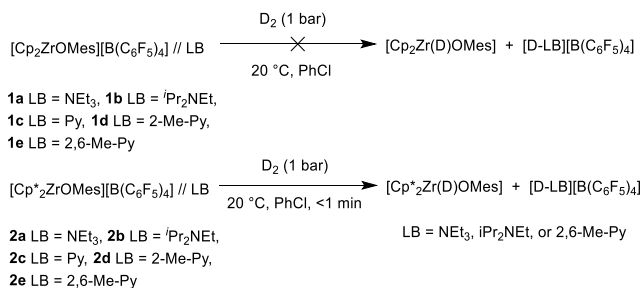
Figure 4. Molecular structures of **2c** (top) and **2d** (bottom), as determined by single crystal X-ray diffraction. Thermal ellipsoids are drawn at the 50% probability level. Hydrogen atoms, the $[B(C_6F_5)_4]^-$ counterion, and PhCl solvent of crystallization are omitted for clarity. Selected bond lengths (Å) and angles (deg): **2c**: Zr1—O1 1.982(2), Zr1—N1 2.326(3), O1—C26 1.375(4), Zr1—O1—C26 158.8(2), Cp*—Zr—Cp* 135.5(7). **2d**: Zr1—O1 1.975(3), Zr1—N1 2.386(4), O1—C21 1.369(5), Zr1—O1—C21 167.4(3), Cp*—Zr—Cp* 132.7(9).

Reactivity of Lewis Pairs with Dihydrogen (D_2)

Initial investigations into the ability of these Zr/N systems to activate small molecules involved reactions with dihydrogen. D_2 was used in place of H_2 to allow for easier reaction monitoring via 2H NMR spectroscopy.

For **1a-e**, no reaction was observed upon addition of D₂ gas (1 bar) to a PhCl solution of the pair (Scheme 3). This is in line with previous work where at least one Cp* ligand was necessary for the reaction to proceed,⁴ and adds credence to the hypothesis that transient binding of H₂ to the Zr center is required for subsequent activation to occur, meaning that simply changing the Lewis base from a phosphine to a nitrogen compound does not seem to have any effect.

Scheme 3. Reactivity of Systems **1a-e** and **2a-e** with D₂ (1 bar)



The reaction proceeded smoothly for Lewis pairs **2a**, **2b**, and **2e** with the characteristic Zr-D singlet appearing in the ²H NMR spectra for each reaction ($\delta = 6.06$ ppm) by the time spectra were recorded (less than 1 minute). For **2a** and **2b** the ²H resonance for the ammonium salts was not seen, as these compounds are insoluble in PhCl. For **2e**, a broad resonance is seen at 12.4 ppm in the ²H spectrum, corresponding to the [C₅H₃(CH₃)₂N-D]⁺ species.

Neither the **2c** or **2d** pairs demonstrated reactivity towards D₂, likely a result of the lower basicity of the Lewis bases, in addition to the more persistent Zr-N interactions as evidenced by DOSY NMR studies.

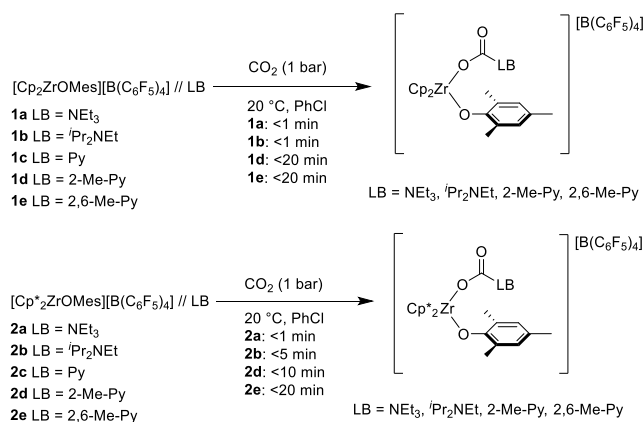
Reactivity of Lewis Pairs with Carbon Dioxide

PhBr-*d*₅ solutions of the Lewis pairs **1a-e** and **2a-e** were exposed to 1 bar CO₂ (Scheme 4). The pairs **1a** and **1b** reacted almost instantly, with both turning much paler yellow. ¹⁵N-HMBC NMR spectra showed new peaks at 446.0 and 446.5 ppm respectively, which were assigned to the CO₂ activated product. No reaction was seen for **1c**; however, both **1d** and **1e** reacted, albeit more

slowly than **1a** and **1b** (<20 min), with the signals at 450.1 and 464.0 ppm respectively in the ^{15}N -HMBC NMR spectra.

Upon addition of CO_2 , **2a** instantly changed color to yellow, with the new resonance in the ^{15}N -HMBC NMR spectrum ($\delta = 343.3$ ppm) assigned to the CO_2 activation product. In the case of **2b** a signal in the ^{15}N -HMBC NMR spectrum could not be obtained, and although a color change suggests reaction, further analysis proved inconclusive. Reactions were also seen for both **2d** and **2e**, with the CO_2 activation products assigned in the ^{15}N -HMBC NMR (**2d**: $\delta = 438.1$ ppm, **2e**: $\delta = 466.1$ ppm). Compound **2c** was found to be inactive for CO_2 activation.

Scheme 4. Reaction of **1a-e** and **2a-e** with CO_2 gas (1 bar)



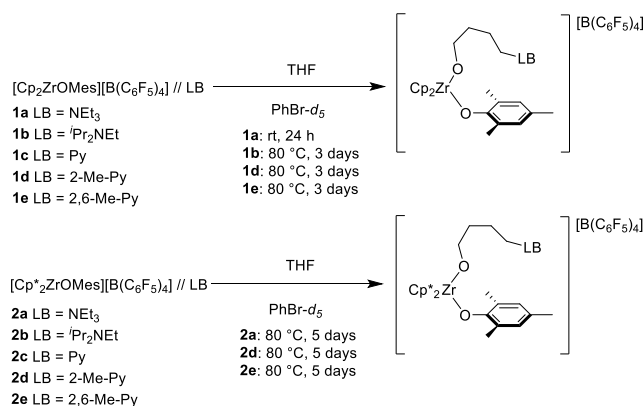
Reactivity of Lewis Pairs with Tetrahydrofuran (THF)

The FLP systems were also tested for their ability to ring-open tetrahydrofuran (THF), with bromobenzene- d_5 solutions of **1a**, **1b**, **1d**, and **1e** undergoing a rapid color change to a bright yellow solution upon addition of THF indicating formation of the Zr-THF adduct (Scheme 5). Formation of the ring-opened products then followed, with the quickest reaction seen for **1a** (24 h). No heating was required for this reaction to reach completion, although some unreacted Zr-THF adduct still remained. Heating at 80 °C for several days resulted in no further conversion. More sluggish reactivity was seen with **1d** and **1e**, with heating at 80 °C over 3 days required for

the reactions to reach completion. **1b** demonstrated much slower reactivity still, with very low conversion (20%) achieved after 3 days at 80 °C and no increase in conversion when left to heat for a further 10 days. No product formed in the reaction of **1c**, although the bound pyridine was eventually displaced by the THF after several days of heating at 80 °C.

Successful reactivity was also seen with **2a**, **2d**, and **2e**, although all of these reactions required much longer timeframes than their Cp counterparts, with 5 days of heating at 80 °C required for the reactions to reach completion. Surprisingly, **2d** was the most reactive of these three samples, achieving the highest yield of 40% (by NMR). **2a** and **2e** had very low yields of 17% and 7% respectively (by NMR), which may be a result of their higher steric bulk being more inhibitory for this reaction when Cp* ligands are present instead of Cp. However, the more electron rich Cp* ligands may also result in comparatively reduced polarization/activation of the bound THF, thereby making subsequent attack from the Lewis base – and consequent ring-opening – less favorable.

Scheme 5. Reactions of **1a-e** and **2a-e** with tetrahydrofuran (THF)



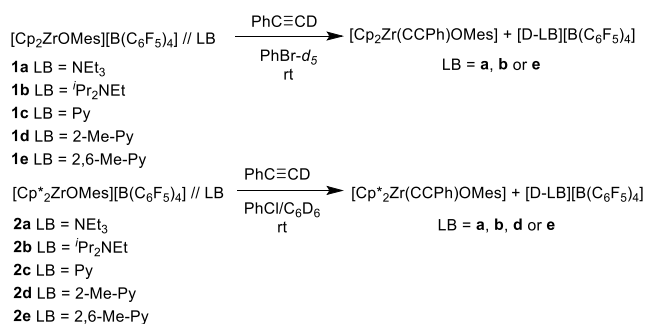
Reactivity of Lewis Pairs with Phenylacetylene-*d*

Reactions of terminal alkynes with FLPs have been shown to proceed via 1,2-addition or deprotonation.³⁶⁻⁴⁰ In this present case, all of the pairs **1a**, **1b**, **1e**, **2a**, **2b**, **2d**, and **2e** react with

phenylacetylene-*d* (PhCCD), via deprotonation of the alkyne (Scheme 6). For **1a**, an instant color change is seen upon addition of PhCCD (to a lighter yellow), followed by the formation of [D-NEt₃][B(C₆F₅)₄] crystals after several minutes and concurrent formation of the zirconium acetylide complex. Both **1b** and **1e** also demonstrate formation of the [D-^{*i*}Pr₂NEt][B(C₆F₅)₄] and [2,6-Me-Py-D][B(C₆F₅)₄] salts, however these reactions are more sluggish (5 min and 30 min respectively). No reaction was seen for **1c** and **1d**. **2a**, **2b**, **2d** and **2e** all reacted successfully with PhCCD, again yielding the deprotonation product.

Less basic, less sterically bulky phosphine Lewis bases have been shown to perform the 1,2-addition reaction previously. The results here suggest harder nitrogen bases are more likely to react via a deprotonation pathway.¹³

Scheme 6. Reaction of FLP systems **1a-e** and **2a-e** with phenylacetylene-*d* (PhCCD)



Catalytic dehydrocoupling of Me₂NH·BH₃

The ability of the Zr/N systems to perform catalysis was tested through the dehydrocoupling of Me₂NH·BH₃. The reactions were monitored by ¹¹B{¹H} NMR spectroscopy, employing a 10 mol% catalyst loading, with the results shown in Table 3. **1a**, **1e** and **2e** achieved complete conversion and >95% yields within 9.5, 10.5 and 7.5 hours respectively, with 2,6-dimethylpyridine the only Lewis base producing high conversions and yields with both cations.

Table 3. Catalytic dehydrocoupling of Me₂NH·BH₃ using FLP systems **1a-e** and **2a-e**.

$$\text{Me}_2\text{NH}\cdot\text{BH}_3 \xrightarrow[\text{PhBr-}d_5]{\text{Zr/N (10 mol\%)}} \frac{1}{2} \begin{array}{c} \text{Me}_2\text{N}-\text{BH}_2 \\ | \quad | \\ \text{H}_2\text{B}-\text{NMe}_2 \end{array}$$

-H₂

| Catalyst | Temperature (°C) | Time (h) | Yield (%) | Conversion (%) |
|-----------|------------------|----------|-----------|----------------|
| 1a | 25 | 9.5 | 97 | 100 |
| 1a | 60 | 0.45 | 93 | 100 |
| 1b | 25 | 14 | 7 | 26 |
| 1c | 25 | 14 | 0 | 0 |
| 1d | 25 | 14 | 9 | 30 |
| 1e | 25 | 7.5 | 79 | 92 |
| 1e | 25 | 10.5 | 96 | 100 |
| 1e | 25 | 14 | 98 | 100 |
| 1e | 60 | 0.5 | 90 | 100 |
| 2a | 25 | 14 | 9 | 10 |
| 2b | 25 | 14 | 13 | 15 |
| 2c | 25 | 14 | 47 | 47 |
| 2d | 25 | 14 | 36 | 42 |
| 2e | 25 | 6.5 | 97 | 100 |
| 2e | 25 | 7.5 | >99 | 100 |
| 2e | 60 | 0.5 | 98 | 100 |

The ability of NEt₃ to catalyze the reaction when combined with **1**, but not with **2**, is in line with previous work which employed phosphines as the Lewis base (P^tBu₃, PCy₃, PEt₃, PPh₃, PMes₃, and P(C₆F₅)₃).¹⁴ The poor performance of **2a** and **2b** is also likely to be a result of the degradation over time; when **2** and **a** or **b** are left together in solution the precipitation of [H-NEt₃][B(C₆F₅)₄] or [H-ⁱPr₂NEt][B(C₆F₅)₄] crystals is observed within a few hours. We were unable to isolate and identify the Zr complex. Increasing reaction temperature to 60 °C improved reaction rates as expected; for **1a**, **1e** and **2e** complete conversion was achieved within 30 min. The pairs **2c-e** are

surprisingly able catalysts for this reaction, outperforming previously reported Zr(IV)-phosphine FLP catalysts.

Using both basicity and steric bulk as rational predictors of reactivity is still difficult. This is highlighted by the fact that P^tBu_3 ($pK_a = 11.4$)⁴¹ was the only phosphine (in combination with **1**) shown to have reactivity similar to **1a**, **1e**, or **2e**; whereas **1b** showed very poor reactivity, despite **b** being more similar to P^tBu_3 in terms of basicity and steric bulk.

The mechanism of these reactions is proposed to follow the same cycle that has been previously reported,⁴² with the same distribution of intermediates seen in the $^{11}B\{^1H\}$ NMR spectra during the reactions (Figure 5). Indeed, examination of the catalytic cycle gives greater clues as to the reason for the varying results seen for each catalyst. The principle role of the Lewis base in the catalytic cycle is currently understood to be the deprotonation of $Me_2NH \cdot BH_3$ (Scheme 7). Therefore, it may be that **1a**, **1e**, and **2e** are more effective at both the deprotonation step, and subsequent dihydrogen release. In the case of **1b**, N,N-diisopropylethylamine may be too bulky to effectively deprotonate $Me_2NH \cdot BH_3$, and the subsequent ammonium salt may be too stable for easy dihydrogen release.

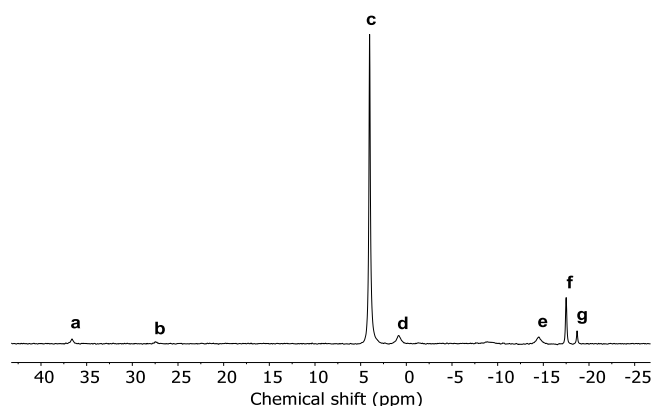
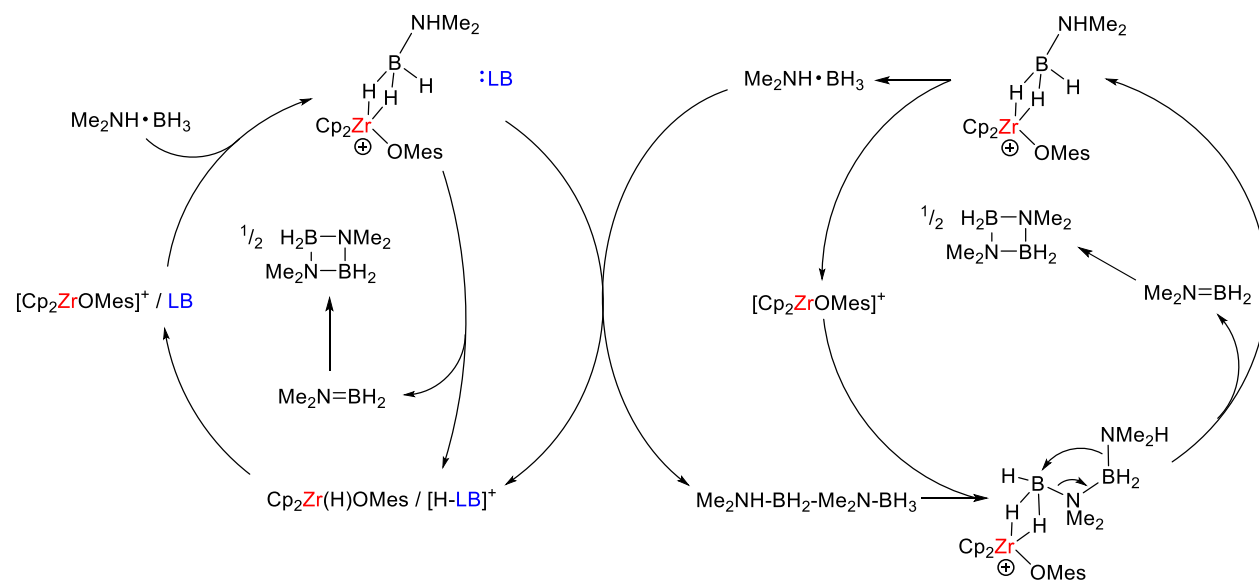


Figure 5. $^{11}B\{^1H\}$ NMR spectrum (160 MHz, 25 °C, $PhBr-d_5$, 7.5 h) for the reaction between $Me_2NH \cdot BH_3$ and 10 mol% **2.1b**. **a** = $Me_2N=BH_2$ (36.6 ppm), **b** = $HB(NMe_2)_2$ (27.5 ppm), **c** =

$[\text{Me}_2\text{N}-\text{BH}_2]_2$ (4.03 ppm), **d** = $\text{Me}_2\text{NH}-\text{BH}_2-\text{Me}_2\text{N}-\text{BH}_3$ (0.82 ppm), **e** = $\text{Me}_2\text{NH}\cdot\text{BH}_3$ and $\text{Me}_2\text{NH}-\text{BH}_2-\text{Me}_2\text{N}-\text{BH}_3$ (-14.5 ppm), **f** = $[\text{B}(\text{C}_6\text{F}_5)_4]^-$ (-17.5 ppm), **g** = $\text{Me}_2\text{N}(\text{B}_2\text{H}_5)$ (-18.7 ppm).

Scheme 7. Proposed reaction mechanism for the catalytic dehydrocoupling of $\text{Me}_2\text{NH}\cdot\text{BH}_3$ using a Zr(IV)/FLP. The $[\text{B}(\text{C}_6\text{F}_5)_4]^-$ counterion has been omitted for clarity.



If we compare the reaction profiles for the reactions of **1a** (Figure 6) and **2e** (Figure 7), it is clear that a larger concentration of $\text{Me}_2\text{NH-BH}_2-\text{Me}_2\text{N-BH}_3$ is present for **1a**. This is one reason for slower product formation and is perhaps a result of the persistence of the ammonium salt in the reaction which, by preventing the release of H_2 through reaction with $\text{Cp}_2\text{Zr(H)OMes}$, means there is less $[\text{Cp}_2\text{ZrOMes}]^+$ available for the conversion of $\text{Me}_2\text{NH-BH}_2-\text{Me}_2\text{N-BH}_3$, thus reducing the rate of product formation and overall catalytic turnover.

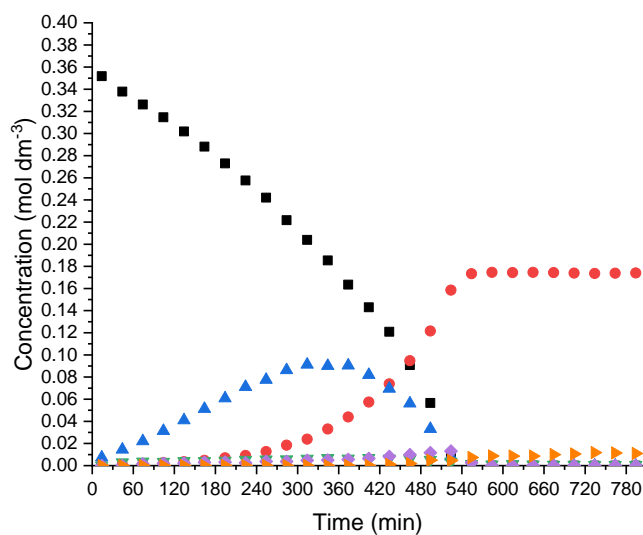


Figure 6. Reaction of **1a** with Me₂NH·BH₃ (25 °C, PhBr-*d*₅, 14 h): (black ■) Me₂NH·BH₃; (red ●) [Me₂N-BH₂]₂; (blue ▲) Me₂NH-BH₂-Me₂N-BH₃; (purple ◆) Me₂N=BH₂; (green ▼) Me₂N(B₂H₅); (orange ►) HB(NMe₂)₂.

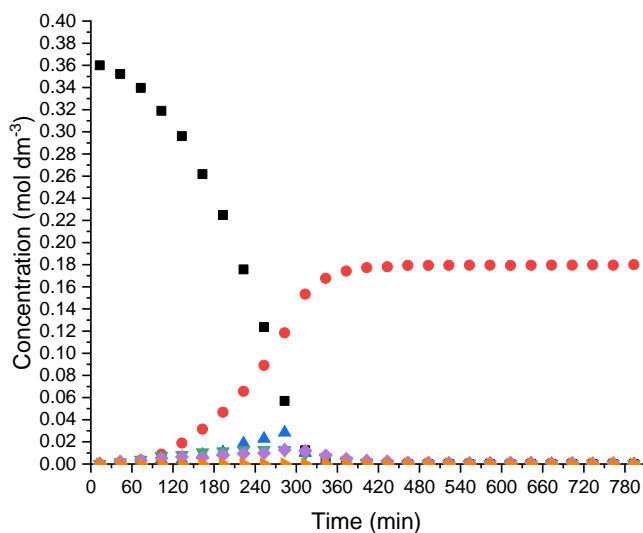


Figure 7. Reaction of **2e** with Me₂NH·BH₃ (25 °C, PhBr-*d*₅, 14 h): (black ■) Me₂NH·BH₃; (red ●) [Me₂N-BH₂]₂; (blue ▲) Me₂NH-BH₂-Me₂N-BH₃; (purple ◆) Me₂N=BH₂; (green ▼) Me₂N(B₂H₅); (orange ►) HB(NMe₂)₂.

CONCLUSION

A range of intermolecular zirconium/nitrogen FLPs have been synthesized through combination of zirconocene cations with either an amine or a pyridine derivative. The nature of the Lewis acid/Lewis base interaction was elucidated through DOSY NMR spectroscopic studies, before the activation of a number of different small molecules was demonstrated. Steric effects once again play an important role, with pyridine (**c**) largely being shown to be an ineffective Lewis base for these reactions. The dehydrocoupling of $\text{Me}_2\text{NH}\cdot\text{BH}_3$ was also achieved, with 2,6-dimethylpyridine and triethylamine shown to be the most effective Lewis bases. These results highlight that the hard-soft mismatch in previous intermolecular Zr(IV)-phosphine FLPs is of little or secondary importance. Given judicious choice of nitrogen base very similar FLP reactivity is observed in these Zr(IV)-amine systems, with steric bulk and basicity remaining the key factors in determining reactivity.

EXPERIMENTAL SECTION

General Considerations

Unless otherwise stated, all manipulations were undertaken under an atmosphere of argon or nitrogen using standard glovebox (M. Braun $\text{O}_2 < 0.1$ ppm, $\text{H}_2\text{O} < 0.1$ ppm) and Schlenk line techniques. All glassware was dried in an oven at 200°C overnight and cooled under vacuum prior to use. The complexes $[\text{Cp}_2\text{ZrOMes}][\text{B}(\text{C}_6\text{F}_5)_4]$ and $[\text{Cp}^*\text{ZrOMes}][\text{B}(\text{C}_6\text{F}_5)_4]$ were synthesized following a literature procedure.¹³ Triethylamine, N,N-diisopropylethylamine, pyridine, 2-methylpyridine, and 2,6-dimethylpyridine were purchased from Sigma-Aldrich and distilled from CaH_2 prior to use. $\text{Me}_2\text{NH}\cdot\text{BH}_3$ was purchased from Sigma-Aldrich and purified by sublimation prior to use (25°C , 2×10^{-2} Torr). Phenylacetylene-*d* was purchased from Sigma-Aldrich and purified by distillation before use. Reagent gases (D_2 and CO_2) were dried prior to using by passing

through a -78 °C trap. THF was purified using a Grubbs type purification system. Chlorobenzene was purchased from Sigma-Aldrich and dried over 4 Å molecular sieves prior to use.

NMR spectra were recorded using Jeol ECS 300 (300 MHz), Bruker Nano 400 (400 MHz), Jeol ECS 400 (400 MHz), Varian VNMRS500 (500 MHz), and Bruker Avance III HD 500 Cryo (500 MHz) spectrometers. ¹⁵N-HMBC NMR spectra are referenced to NH₃. Deuterated solvents were obtained from Sigma-Aldrich (benzene-*d*₆, bromobenzene-*d*₅, and acetonitrile-*d*₃) and distilled from CaH₂ or dried over 4 Å molecular sieves prior to use. Spectra of air-sensitive compounds were recorded using NMR tubes fitted with J. Young valves. Spectra of boron-containing compounds were obtained using quartz NMR tubes fitted with J. Young valves.

X-ray diffraction experiments on **2c** and **2d** were carried out at 100(2) K on a Bruker APEX II diffractometer using Mo-K_α radiation ($\lambda = 0.71073$ Å). See the Supporting Information for further details.

Mass spectrometry experiments were carried out by the University of Bristol Mass Spectrometry Service on a Bruker Daltronics MicrOTOF II with a TOF analyzer or a Waters Synapt G2S with an IMS-Q-TOF analyzer. All samples were run in pre-dried PhCl or CH₃CN.

Generation of FLPs [*Cp*₂ZrOMes][*B*(*C*₆*F*₅)₄] // LB (1a-e**)**

In a glovebox, **1** (30 mg, 0.029 mmol) was dissolved in bromobenzene-*d*₅ (0.5 mL) before the Lewis base (**a** = NEt₃ (4.1 μL, 0.029 mmol), **b** = ⁱPr₂NEt (5.1 μL, 0.029 mmol), **c** = pyridine (2.4 μL, 0.029 mmol), **d** = 2-methylpyridine (2.9 μL, 0.029 mmol), **e** = 2,6-dimethylpyridine (3.4 μL, 0.029 mmol)) was added. A color change (orange to yellow) was observed in each case.

The FLP was then used in situ for reactions with substrates, without isolation.

1a. ¹H NMR (500 MHz, PhBr-*d*₅) δ 6.75 (2H, s, *m*-Ar*H*), 6.10 (10H, s, Cp), 2.36 (6H, q, ³*J*_{HH} = 7.2 Hz, N(CH₂CH₃)₃), 2.20 (3H, s, *p*-Ar-CH₃), 1.86 (6H, s, *o*-Ar-CH₃), 0.80 (9H, t, ³*J*_{HH} = 7.2 Hz,

N(CH₂CH₃)₃) ppm. ¹⁵N-HMBC NMR (500 MHz, 51 MHz, PhBr-*d*₅) δ 163.5 (Zr-NEt₃) ppm. NB: NEt₃ δ = 47.6 ppm.

1b. ¹H NMR (500 MHz, PhBr-*d*₅) δ 6.75 (2H, s, *m*-ArH), 6.10 (10H, s, Cp), 2.90 (2H, sept, ³J_{HH} = 6.5 Hz, N(CH(CH₃)₂)₂), 2.37 (2H, q, ³J_{HH} = 7.2 Hz, NCH₂CH₃), 2.19 (3H, s, *p*-Ar-CH₃), 1.86 (6H, s, *o*-Ar-CH₃), 1.04-0.58 (15H, br, CH₃CH₂N(CH(CH₃)₂)₂) ppm. ¹⁵N-HMBC NMR (500 MHz, 51 MHz, PhBr-*d*₅) δ 185.5 (Zr-N(^{*i*}Pr)₂Et) ppm. NB: ^{*i*}Pr₂NEt δ = 57.5 ppm.

1c. ¹H NMR (500 MHz, PhBr-*d*₅) δ 8.19 (2H, m, *o*-PyH), 7.46 (1H, m, *m*-PyH), 7.10 (2H, m, *p*-PyH), 6.73 (2H, s, *m*-ArH), 5.97 (10H, s, Cp), 2.18 (3H, s, *p*-Ar-CH₃), 1.79 (6H, s, *o*-Ar-CH₃) ppm. ¹⁵N-HMBC NMR (500 MHz, 51 MHz, PhBr-*d*₅) signal not seen for FLP (see Results and Discussion). NB: Pyridine δ = 318.9 ppm.

1d. ¹H NMR (500 MHz, PhBr-*d*₅) δ 8.62 (1H, br, *o*-PyH), 7.96 (1H, m, *p*-PyH), 7.40 (2H, m, *m*-PyH), 6.74 (2H, s, *m*-ArH), 5.99 (10H, s, Cp), 2.18 (3H, s, *p*-Ar-CH₃), 2.11 (3H, br, *o*-Py-CH₃), 1.83 (6H, s, *o*-Ar-CH₃) ppm. ¹⁵N-HMBC NMR (500 MHz, 51 MHz, PhBr-*d*₅) δ 302.1 (Zr-NC₅H₄CH₃) ppm. NB: 2-methylpyridine δ = 317.7 ppm.

1e. ¹H NMR (500 MHz, PhBr-*d*₅) δ 7.25 (1H, t, ³J_{HH} = 7.7 Hz, *p*-PyH), 6.81 (2H, m, *m*-PyH), 6.71 (2H, s, *m*-ArH), 6.02 (10H, s, Cp), 2.27 (6H, s, *o*-Py-CH₃), 2.16 (3H, s, *p*-Ar-CH₃), 1.72 (6H, s, *o*-ArH-CH₃) ppm. ¹⁵N-HMBC NMR (500 MHz, 51 MHz, PhBr-*d*₅) δ 249.8 (Zr-NC₅H₃(CH₃)₂) ppm. NB: 2,6-dimethylpyridine δ = 317.2 ppm.

[Cp*₂ZrOMes][B(C₆F₅)₄] // LB (**2a-e**)

In a glovebox, **2** (34.1 mg, 0.029 mmol) was dissolved in bromobenzene-*d*₅ (0.5 mL) before the Lewis base (**a** = NEt₃ (4.1 μL, 0.029 mmol), **b** = ^{*i*}Pr₂NEt (5.1 μL, 0.029 mmol), **c** = pyridine (2.4 μL, 0.029 mmol), **d** = 2-methylpyridine (2.9 μL, 0.029 mmol), **e** = 2,6-dimethylpyridine (3.4 μL,

0.029 mmol)) was added. A color change (dark orange to red) was observed for **a**, **b** and **e**. The solution turned green upon addition of **c**, and slightly lightened in color upon addition of **d**.

The FLP was then used in situ for reactions with substrates, without isolation. However, crystals of **2c**, and **2d** suitable for X-ray crystallography were obtained by layering a PhCl solution of **2c**, and a PhBr-*d*₅ solution of **2d** with pentane.

2a. ¹H NMR (500 MHz, PhCl-*d*₅) δ 6.79 (2H, s, *m*-ArH), 2.37 (6H, q, ³*J*_{HH} = 7.2 Hz, N(CH₂CH₃)₃), 2.20 (3H, s, *p*-Ar-CH₃), 1.73 (6H, s, *o*-Ar-CH₃), 1.64 (30H, s, Cp*), 0.82 (9H, t, ³*J*_{HH} = 7.2 Hz, N(CH₂CH₃)₃) ppm. ¹⁵N-HMBC NMR (500 MHz, 51 MHz, PhBr-*d*₅) δ 54.2 (Zr-NEt₃) ppm. NB: NEt₃ δ = 47.6 ppm.

2b. ¹H NMR (500 MHz, PhBr-*d*₅) δ 6.78 (2H, s, *m*-ArH), 2.91 (2H, sept., ³*J*_{HH} = 6.5 Hz, N(CH(CH₃)₂)₂), 2.37 (2H, q, ³*J*_{HH} = 7.2 Hz, NCH₂CH₃), 2.20 (3H, s, *p*-Ar-CH₃), 1.73 (6H, s, *o*-Ar-CH₃), 1.64 (30H, s, Cp*), 1.05-0.63 (15H, br, CH₃CH₂N(CH(CH₃)₂)₂) ppm. ¹⁵N-HMBC NMR (500 MHz, 51 MHz, PhBr-*d*₅) signal not seen for FLP (see Results and Discussion).

2c. ¹H NMR (500 MHz, PhBr-*d*₅) δ 8.55 (1H, br, *o*-ArH), 8.38 (1H, br, *o*-ArH), 7.32 (1H, br, *p*-ArH), 7.07-6.97 (2H, m, *m*-ArH(Py)), 6.78 (1H, s, *m*-ArH(Mes)), 6.67 (1H, s, *m*-ArH(Mes)), 2.17 (3H, s, *p*-Ar-CH₃), 1.94 (3H, s, *o*-Ar-CH₃), 1.89 (3H, s, *o*-Ar-CH₃), 1.47 (30H, s, Cp*) ppm. ¹³C NMR (125 MHz, PhBr-*d*₅) δ 156.4 (s, *i*-C), 151.7 (s, *o*-CH(Py)), 138.2 (s, *p*-CH(Py)), 130.7 and 130.2 (s, *m*-CH(Mes)), 126.5 (s, *o*-CCH₃(Mes)), 125.8 (s, Cp*), 123.6 (s, *p*-CCH₃(Mes)), 21.7 and 20.4 (s, *o*-CH₃), 19.42 (s, *p*-CH₃), 11.5 (s, Cp*-Me) ppm. Remaining peaks obscured by PhBr-*d*₅ solvent. ¹⁵N-HMBC NMR (500 MHz, 51 MHz, PhBr-*d*₅) δ 260.5 (Zr-Py) ppm. NB: Pyridine δ = 318.9 ppm. ESI-MS (+ve detection) 574.2645 *m/z*.

2d. ¹H NMR (500 MHz, PhBr-*d*₅) δ 7.94 (1H, br, *o*-ArH), 7.41 (1H, m, *p*-ArH), 7.16-7.12 (2H, m, *m*-ArH(Py)), 6.73 and 6.71 (2H, s, *m*-ArH(Mes)), 2.20 (3H, s, *o*-Ar-CH₃(Py)), 2.16 (3H, s, *p*-

Ar-CH₃), 1.99 (3H, s, *o*-Ar-CH₃(Mes)), 1.78 (3H, s, *o*-Ar-CH₃(Mes)), 1.51 (30H, s, Cp*) ppm. ¹³C NMR (125 MHz, PhBr-*d*₅) δ 155.8 (s, *o*-CCH₃(Py)), 148.4 (s, *o*-CH(Py)), 134.2 (s, *p*-CH(Py)), 128.6 (s, Cp*), 26.1 (s, *o*-CH₃(Py)), 20.8 and 20.4 (s, *o*-CH₃(Mes)), 19.3 (s, *p*-CH₃), 12.0 (s, Cp*-Me) ppm. Remaining peaks obscured by PhBr-*d*₅ solvent. ¹⁵N-HMBC NMR (500 MHz, 51 MHz, PhBr-*d*₅) δ 261.1 (Zr-NC₅H₄(CH₃)) ppm. NB: 2-methylpyridine δ = 317.7 ppm.

2e. ¹H NMR (500 MHz, PhBr-*d*₅) δ 7.23 (1H, t, ³*J*_{HH} = 7.8 Hz, *p*-PyH), 6.79 (2H, s, *m*-ArH), 6.72 (2H, m, *m*-PyH), 2.30 (6H, s, *o*-Py-CH₃), 2.20 (3H, s, *p*-Ar-CH₃), 1.73 (6H, s, *o*-Ar-CH₃), 1.63 (30H, s, Cp*) ppm. ¹⁵N-HMBC NMR (500 MHz, 51 MHz, PhBr-*d*₅) δ 286.0 (Zr-NC₅H₃(CH₃)₂) ppm. NB: 2,6-dimethylpyridine δ = 317.2 ppm.

DOSY studies of **1a-e** and **2a-e**

Samples of **1a-e** and **2a-e** and separate control samples of **a-e** were made as detailed above. ¹H DOSY NMR spectroscopy were carried out using 15 increments and a diffusion delay of 100 ms. The results of the study can be found in the Supporting Information. All data were analyzed using MestReNova.

Reactions of Pairs with D₂

Reactivity of [Cp₂ZrOMes][B(C₆F₅)₄] // LB (**1a-e**)

In a glovebox, **1** (30 mg, 0.029 mmol) was dissolved in PhCl (0.5 mL) in an NMR tube fitted with a J. Youngs valve, before C₆D₆ (one drop) was added for reference in ²H NMR spectra. An equimolar amount of the Lewis base (**a** = NEt₃ (4.1 μL, 0.029 mmol), **b** = ^{*i*}Pr₂NEt (5.1 μL, 0.029 mmol), **c** = pyridine (2.4 μL, 0.029 mmol), **d** = 2-methylpyridine (2.9 μL, 0.029 mmol), **e** = 2,6-dimethylpyridine (3.4 μL, 0.029 mmol)) was then added. Outside of the glovebox, the sample was degassed twice via freeze-pump-thaw, before being refilled with D₂ gas (1 bar). In all cases, no change in the NMR spectra was seen.

*Reactivity of [Cp*₂ZrOMes][B(C₆F₅)₄] // LB (2a-e)*

In a glovebox, **2** (34.1 mg, 0.029 mmol) was dissolved in PhCl (0.5 mL) in an NMR tube fitted with a J. Youngs valve, before C₆D₆ (one drop) was added for reference in ²H NMR spectra. An equimolar amount of the Lewis base (**a** = NEt₃ (4.1 μL, 0.029 mmol), **b** = ⁱPr₂NEt (5.1 μL, 0.029 mmol), **c** = pyridine (2.4 μL, 0.029 mmol), **d** = 2-methylpyridine (2.9 μL, 0.029 mmol), **e** = 2,6-dimethylpyridine (3.4 μL, 0.029 mmol)) was then added. Outside of the glovebox, the sample was degassed twice via freeze-pump-thaw, before being refilled with D₂ gas (1 bar). A color change from red to yellow was seen for **2a**, **2b**, and **2e**. Collected spectral data are detailed below:

2a + D₂. ²H NMR (77 MHz, PhCl/C₆D₆) δ 6.06 (s, Zr-*D*) ppm.

2b + D₂. ²H NMR (77 MHz, PhCl/C₆D₆) δ 6.06 (s, Zr-*D*) ppm.

2e + D₂. ²H NMR (77 MHz, PhCl/C₆D₆) δ 12.4 (br, N-*D*), 6.06 (s, Zr-*D*) ppm.

Reactions of Pairs with CO₂

Reactivity of [Cp₂ZrOMes][B(C₆F₅)₄] // LB (1a-e)

In a glovebox, **1** (30 mg, 0.029 mmol) was dissolved in PhBr-*d*₅ (0.5 mL) in an NMR tube fitted with a J. Youngs valve. An equimolar amount of the Lewis base (**a** = NEt₃ (4.1 μL, 0.029 mmol), **b** = ⁱPr₂NEt (5.1 μL, 0.029 mmol), **c** = pyridine (2.4 μL, 0.029 mmol), **d** = 2-methylpyridine (2.9 μL, 0.029 mmol), **e** = 2,6-dimethylpyridine (3.4 μL, 0.029 mmol)) was then added. Outside of the glovebox, the sample was degassed twice via freeze-pump-thaw, before being refilled with CO₂ gas (1 bar) via a -78 °C trap. **1a**, **1b**, and **1d** showed a lightening in color, whereas **1e** showed no clear color change. Isolation of any products was attempted but not possible, and so all spectral data were obtained in situ. **1c** did not react.

1a + CO₂. ¹H NMR (500 MHz, PhBr-*d*₅) δ 6.85 (2H, s, *m*-Ar*H*), 6.17 (10H, s, Cp), 2.37 (6H, q, N(CH₂CH₃)₃), 2.28 (3H, s, *p*-Ar-CH₃), 2.23 (6H, s, *o*-Ar-CH₃), 0.80 (9H, t, N(CH₂CH₃)₃) ppm.

^{13}C NMR (125 MHz, PhBr- d_5) δ 165.3 (s, C(O)=O), 161.8 (s, *i*-C), 128.6 (s, *o*-C), 126.5 (s, *m*-C), 124.6 (s, *p*-C), 112.9 (s, Cp), 47.0 (s, N(CH₂CH₃)₃), 20.9 (s, *p*-CH₃), 18.6 (s, *o*-CH₃), 10.5 (s, N(CH₂CH₃)₃) ppm. ^{15}N -HMBC NMR (500 MHz, 51 MHz, PhBr- d_5) δ 446.0 (Zr-CO₂-NEt₃) ppm.

1b + CO₂. ^1H NMR (500 MHz, PhBr- d_5) δ 6.85 (2H, s, *m*-ArH), 6.17 (10H, s, Cp), 2.92 (2H, sept., N(CH(CH₃)₂)₂), 2.38 (2H, q, NCH₂CH₃), 2.28 (3H, s, *p*-Ar-CH₃), 2.23 (6H, s, *o*-Ar-CH₃), 1.00-0.65 (15H, br, CH₃CH₂N(CH(CH₃)₂)₂) ppm. ^{13}C NMR (125 MHz, PhBr- d_5) δ 168.2 (s, C(O)=O), 161.8 (s, *i*-C), 128.6 (s, *o*-C), 126.5 (s, *m*-C), 124.7 (s, *p*-C), 112.9 (s, Cp), 56.0 (s, N(CH(CH₃)₂)₂), 43.4 (s, NCH₂CH₃), 21.0 (s, N(CH(CH₃)₂)₂), 20.7 (s, *p*-CH₃), 18.7 (s, *o*-CH₃), 16.6 (s, NCH₂CH₃) ppm. ^{15}N -HMBC NMR (500 MHz, 51 MHz, PhBr- d_5) δ 446.5 (Zr-CO₂-N(^{*i*}Pr)₂Et) ppm.

1d + CO₂. ^1H NMR (500 MHz, PhBr- d_5) δ 8.62 (1H, br, *o*-PyH), 7.82 (1H, m, *p*-PyH), 7.44 (2H, m, *m*-PyH), 6.85 (2H, s, *m*-ArH), 6.17 (10H, s, Cp), 2.28 (3H, s, *p*-Ar-CH₃), 2.17 (6H, s, *o*-Ar-CH₃), 2.10 (3H, br, *o*-Py-CH₃) ppm. ^{13}C NMR (125 MHz, PhBr- d_5) δ 161.6 (s, C(O)=O), 160.9 (s, *i*-C), 155.0 (s, *o*-CCH₃(Py)), 142.5 (s, *o*-CH(Py)), 134.0 (s, *p*-C(Py)), 128.4 (s, *o*-C(Mes)), 126.3 (s, *m*-C(Mes)), 124.7 (s, *p*-C(Mes)), 124.4 (s, *m*-C(Py)), 123.0 (s, *m*-C(Py)), 112.7 (s, Cp), 25.4 (s, *o*-CH₃(Py)), 20.6 (s, *p*-CH₃), 18.4 (s, *o*-CH₃(Mes)) ppm. ^{15}N -HMBC NMR (500 MHz, 51 MHz, PhBr- d_5) δ 450.1 (Zr-CO₂-NC₅H₄CH₃) ppm.

1e + CO₂. ^1H NMR (500 MHz, PhBr- d_5) δ 7.33 (1H, t, $^3J_{\text{HH}} = 7.7$ Hz, *p*-PyH), 6.79 (2H, m, *m*-PyH), 6.74 (2H, s, *m*-ArH), 6.14 (10H, s, Cp), 2.37 (3H, s, *p*-Ar-CH₃), 2.15 (6H, s, *o*-ArH-CH₃), 2.12 (6H, s, *o*-Py-CH₃) ppm. ^{13}C NMR (125 MHz, PhBr- d_5) δ 160.9 (s, C(O)=O), 160.5 (s, *i*-C), 155.4 (s, *o*-C(Py)), 140.0 (s, *p*-C(Py)), 128.6 (s, *o*-C(Mes)), 126.5 (s, *m*-C(Mes)), 124.7 (s, *p*-C(Mes)), 115.6 (s, Cp), 34.2 (s, *o*-CH₃(Py)), 21.6 (s, *p*-CH₃), 17.7 (s, *o*-CH₃(Mes)) ppm.

Remaining peaks obscured by PhBr-*d*₅ solvent. ¹⁵N-HMBC NMR (500 MHz, 51 MHz, PhBr-*d*₅) δ 464.0 (Zr-CO₂-NC₅H₃(CH₃)₂) ppm.

*Reactivity of [Cp*₂ZrOMes][B(C₆F₅)₄] // LB (2a-e)*

In a glovebox, **2** (34.1 mg, 0.029 mmol) was dissolved in PhBr-*d*₅ (0.5 mL) in an NMR tube fitted with a J. Youngs valve. An equimolar amount of the Lewis base (**a** = NEt₃ (4.1 μ L, 0.029 mmol), **b** = ^{*i*}Pr₂NEt (5.1 μ L, 0.029 mmol), **c** = pyridine (2.4 μ L, 0.029 mmol), **d** = 2-methylpyridine (2.9 μ L, 0.029 mmol), **e** = 2,6-dimethylpyridine (3.4 μ L, 0.029 mmol)) was then added. Outside of the glovebox, the sample was degassed twice via freeze-pump-thaw, before being refilled with CO₂ gas (1 bar) via a -78 °C. A color change from to yellow was seen for **2a**, **2b**, **2d**, and **2e**. Isolation of any products was attempted but not possible, and so all spectral data were obtained in situ. **2c** did not react.

2a + CO₂. ¹H NMR (500 MHz, PhBr-*d*₅) δ 6.71 (2H, s, *m*-ArH), 2.33 (6H, q, N(CH₂CH₃)₃), 2.15 (3H, s, *p*-Ar-CH₃), 1.94 (6H, s, *o*-Ar-CH₃), 1.83 (30H, s, Cp*), 0.75 (9H, t, N(CH₂CH₃)₃) ppm. ¹³C NMR (125 MHz, PhCl) δ 162.7 (s, C(O)=O), 156.7 (s, *i*-C), 124.6 (s, *o*-C), 123.2 (s, *p*-C), 121.7 (s, Cp*), 46.9 (s, N(CH₂CH₃)₃), 20.3 (s, *p*-CH₃), 16.9 (s, *o*-CH₃), 10.9 (s, N(CH₂CH₃)₃), 9.4 (s, Cp*) ppm. ¹⁵N-HMBC NMR (500 MHz, 51 MHz, PhBr-*d*₅) δ 343.3 (Zr-CO₂-NEt₃) ppm.

2b + CO₂. ¹H NMR (500 MHz, PhBr-*d*₅) δ 6.80 (2H, s, *m*-ArH), 2.91 (2H, br, N(CH(CH₃)₂)₂), 2.38 (2H, q, ³J_{HH} = 7.2 Hz, NCH₂CH₃), 2.16 (3H, s, *p*-Ar-CH₃), 1.90 (6H, s, *o*-Ar-CH₃), 1.83 (30H, s, Cp*), 1.00-0.74 (15H, br, CH₃CH₂N(CH(CH₃)₂)₂) ppm. ¹³C NMR (125 MHz, PhBr-*d*₅) δ 161.4 (s, C(O)=O), 155.9 (s, *i*-C), 124.7 (s, *o*-C), 123.1 (s, *p*-C), 56.1 (s, N(CH(CH₃)₂)₂), 43.5 (s, NCH₂CH₃), 21.1 (s, N(CH(CH₃)₂)₂), 22.6 (s, *p*-CH₃), 18.4 (s, *o*-CH₃), 16.7 (s, NCH₂CH₃), 11.3 (s, Cp*) ppm. Remaining NMR peaks obscured by solvent. ¹⁵N-HMBC NMR (500 MHz, 51 MHz, PhBr-*d*₅) signal not seen (see Results and Discussion).

2d + CO₂. ¹H NMR (500 MHz, PhBr-*d*₅) δ 7.65 (1H, m, *p*-PyH), 7.47 (1H, m, *m*-PyH), 6.97-6.90 (2H, m, Py), 6.52 (2H, s, *m*-ArH), 6.17 (10H, s, Cp), 2.22 (3H, s, *p*-Ar-CH₃), 2.16 (3H, br, *o*-Py-CH₃), 1.88 (30H, s, Cp*), 1.75 (6H, s, *o*-Ar-CH₃), ppm. ¹⁵N-HMBC NMR (500 MHz, 51 MHz, PhBr-*d*₅) δ 438.1 (Zr-CO₂-NC₅H₄CH₃) ppm.

2e + CO₂. ¹H NMR (500 MHz, PhBr-*d*₅) δ 7.30 (1H, t, ³J_{HH} = 7.8 Hz, *p*-PyH), 6.80 (2H, s, *m*-ArH), 6.74 (2H, m, *m*-PyH), 2.18 (6H, s, *o*-Py-CH₃), 1.89 (3H, s, *p*-Ar-CH₃), 1.81 (30H, s, Cp*), 1.76 (6H, s, *o*-Ar-CH₃) ppm. ¹⁵N-HMBC NMR (500 MHz, 51 MHz, PhBr-*d*₅) δ 466.1 (Zr-CO₂-NC₅H₃(CH₃)₂) ppm.

Reactions of Pairs with Tetrahydrofuran (THF)

Reactivity of [Cp₂ZrOMes][B(C₆F₅)₄] // LB (**1a-e**)

In a glovebox, **1** (30 mg, 0.029 mmol) was dissolved in PhBr-*d*₅ (0.5 mL) in an NMR tube fitted with a J. Youngs valve. An equimolar amount of the Lewis base (**a** = NEt₃ (4.1 μL, 0.029 mmol), **b** = ^{*i*}Pr₂NEt (5.1 μL, 0.029 mmol), **c** = pyridine (2.4 μL, 0.029 mmol), **d** = 2-methylpyridine (2.9 μL, 0.029 mmol), **e** = 2,6-dimethylpyridine (3.4 μL, 0.029 mmol)) was then added. Tetrahydrofuran (THF, 2.4 μL, 0.029 mmol) was then added, with **1a**, **1b**, **1d**, and **1e** all forming yellow solutions (already yellow solutions darkened slightly). **1a** was left to react at room temperature for 24 h, all other reactions were heated to 80 °C for 3 days. Where sufficient quantities of product were present, the sample was precipitated out into stirring hexane, before being washed twice with hexane (2 × 1 mL) and once with pentane (1 mL) before being dried in vacuo.

1a + THF. Yield = 28.9 mg, 82%. ¹H NMR (400 MHz, PhBr-*d*₅): δ 6.80 (2H, s, Ar-H), 6.07 (10H, s, Cp), 3.90 (2H, m, α-CH₂), 2.50 (2H, m, δ-CH₂), 2.43 (6H, q, ³J_{HH} = 7 Hz, N(CH₂CH₃)₃), 2.22 (3H, s, *p*-CH₃), 2.12 (6H, s, *o*-CH₃), 1.31 (4H, m, β-CH₂ and γ-CH₂), 0.68 (9H, m,

N(CH₂CH₃)₃) ppm. ¹³C NMR (125 MHz, PhBr-*d*₅): δ 161.0 (s, *i*-C), 127.4 (s, *o*-C), 124.6 (s, *p*-C), 112.8 (s, Cp), 71.9 (s, α-CH₂), 48.1 (s, β-CH₂), 30.5 (s, γ-CH₂), 20.8 (s, *p*-CH₃), 18.5 (s, δ-CH₂), 17.9 (s, *o*-CH₃), 11.8 (s, N(CH₂CH₃)), 6.73 (s, N(CH₂CH₃)) ppm. Remaining peaks obscured by PhBr-*d*₅ solvent. ¹⁵N-HMBC NMR (500 MHz, 51 MHz, PhBr-*d*₅): δ 337.5 (-CH₂N⁺Et₃) ppm. ESI-MS (+ve detection) 528.2422 *m/z* [M]⁺, 174.1930 *m/z* [HO(C₄H₈)NEt₃]⁺.

1b + THF. Yield = 17% (by NMR). Not enough product to isolate. ¹⁵N-HMBC (500 MHz, 51 MHz, PhBr-*d*₅): δ 315.8 ppm. ESI-MS (+ve detection) 556.2742 *m/z* [M]⁺, 202.2217 *m/z* [HO(C₄H₈)N(^{*i*}Pr)₂Et]⁺.

1d + THF. Yield = 15.8 mg, 45%. ¹H NMR (400 MHz, PhBr-*d*₅): δ 7.65 (1H, m, *o*-ArH), 7.50-7.39 (1H, m, *p*-ArH), 6.99-6.86 (2H, m, *m*-ArH(Py)), 6.80 (2H, s, Ar-H(Mes)), 6.05 (10H, s, Cp), 3.93-3.85 (4H, m, α-CH₂ and δ-CH₂), 2.23 (3H, s, *p*-CH₃), 2.17 (3H, s, *o*-CH₃(Py)), 2.09 (6H, s, *o*-CH₃), 1.65 (2H, m, β-CH₂), 1.35 (2H, m, γ-CH₂) ppm. ¹³C NMR (125 MHz, PhBr-*d*₅): δ 160.1 (s, *i*-C(Mes)), 154.6 (s, *o*-CCH₃(Py)), 141.5 (s, *p*-CH(Py)), 127.4 (s, *o*-CCH₃(Mes)), 125.6 (s, *m*-CH(Py)), 124.6 (s, *p*-CCH₃(Mes)), 123.6 (s, *m*-CH(Py)), 112.8 (s, Cp), 72.0 (s, α-CH₂), 34.3 (s, β-CH₂), 30.3 (s, γ-CH₂), 27.3 (s, *o*-CH₃(Py)), 20.8 (s, *p*-CH₃(Mes)), 19.4 (s, δ-CH₂), 17.9 (s, *o*-CH₃(Mes)) ppm. Remaining aromatic peaks obscured by PhBr-*d*₅ solvent. ¹⁵N-HMBC NMR (500 MHz, 51 MHz, PhBr-*d*₅): δ 411.6 ppm. ESI-MS (+ve detection) 520.1796 *m/z* [M]⁺, 166.1275 *m/z* [HO(C₄H₈)N(CH₃)C₆H₄]⁺.

1e + THF. Yield = 23 mg, 65%. ¹H NMR (400 MHz, PhBr-*d*₅): δ 7.37 (1H, t, ³J_{HH} = 8 Hz, *p*-ArH), 6.82-6.72 (2H, m, *m*-ArH(Py)), 6.80 (2H, s, Ar-H(Mes)), 6.05 (10H, s, Cp), 3.93 (2H, t, ³J_{HH} = 6 Hz, α-CH₂), 3.85 (2H, m, δ-CH₂), 2.26 (6H, s, *o*-CH₃(Py)), 2.23 (3H, s, *p*-CH₃), 2.10 (6H, s, *o*-CH₃), 1.58 (2H, m, β-CH₂), 1.45 (2H, m, γ-CH₂) ppm. ¹³C NMR (125 MHz, PhBr-*d*₅): δ 161.0 (s, *i*-C(Mes)), 154.3 (s, *o*-CCH₃(Py)), 143.8 (s, *p*-CH(Py)), 127.4 (s, *o*-CCH₃(Mes)), 124.6 (s, *p*-

CCH₃(Mes)), 124.0 (s, *m*-CH(Py)), 112.8 (s, Cp), 71.8 (s, α -CH₂), 34.3 (s, β -CH₂), 30.7 (s, γ -CH₂), 25.6 (s, *o*-CH₃(Py)), 20.8 (s, *p*-CH₃(Mes)), 19.8 (s, δ -CH₂), 17.9 (s, *o*-CH₃(Mes)) ppm. Remaining aromatic peaks obscured by PhBr-*d*₅ solvent. ¹⁵N-HMBC (500 MHz, 51 MHz, PhBr-*d*₅): δ 411.8 ppm. ESI-MS (+ve detection) 534.1938 *m/z* [M]⁺, 180.1436 *m/z* [HO(C₄H₈)N(CH₃)₂C₆H₃]⁺.

*Reactivity of [Cp*₂ZrOMes][B(C₆F₅)₄] // LB (2a-e)*

In a glovebox, **2** (34 mg, 0.029 mmol) was dissolved in PhBr-*d*₅ (0.5 mL) in an NMR tube fitted with a J. Youngs valve. An equimolar amount of the Lewis base (**a** = NEt₃ (4.1 μ L, 0.029 mmol), **b** = ^{*i*}Pr₂NEt (5.1 μ L, 0.029 mmol), **c** = pyridine (2.4 μ L, 0.029 mmol), **d** = 2-methylpyridine (2.9 μ L, 0.029 mmol), **e** = 2,6-dimethylpyridine (3.4 μ L, 0.029 mmol)) was then added. Tetrahydrofuran (THF, 2.4 μ L, 0.029 mmol) was then added, with **2a**, **2d**, and **2e** all forming yellow solutions. The reactions were heated at 80 °C for 5 days. Isolation of the products was not possible.

2a + THF. Yield = 17% (by NMR). ¹⁵N-HMBC (500 MHz, 51 MHz, PhBr-*d*₅): δ 341.4 ppm. ESI-MS (+ve detection) 668.3975 *m/z* [M+H]⁺, 174.1888 *m/z* [HO(C₄H₈)NEt₃]⁺.

2d + THF. Yield = 40% (by NMR). ¹⁵N-HMBC (500 MHz, 51 MHz, PhBr-*d*₅): δ 411.3 ppm. ESI-MS (+ve detection) 660.3350 *m/z* [M+H]⁺, 166.1277 *m/z* [HO(C₄H₈)N(CH₃)C₆H₄]⁺.

2e + THF. Yield = 7% (by NMR). Too little product for ¹⁵N-HMBC NMR. ESI-MS (+ve detection) 674.3501 *m/z* [M+H]⁺, 180.1418 *m/z* [HO(C₄H₈)N(CH₃)₂C₆H₃]⁺.

Reaction of Pairs with Phenylacetylene-*d* (PhCCD)

Reactivity of [Cp₂ZrOMes][B(C₆F₅)₄] // LB (1a-e)

In a glovebox, **1** (30 mg, 0.029 mmol) was dissolved in PhBr-*d*₅ (0.5 mL) in an NMR tube fitted with a J. Youngs valve. An equimolar amount of the Lewis base (**a** = NEt₃ (4.1 μ L, 0.029 mmol), **b** = ^{*i*}Pr₂NEt (5.1 μ L, 0.029 mmol), **c** = pyridine (2.4 μ L, 0.029 mmol), **d** = 2-methylpyridine (2.9

μL , 0.029 mmol), **e** = 2,6-dimethylpyridine (3.4 μL , 0.029 mmol)) was then added. Excess phenylacetylene-*d* (3 drops) was then added, resulting in a lightening of the yellow color for **1a** and **1b**, with no color change seen for the reactions of **1c-e**. Neither **1c** nor **1d** demonstrated any reactivity. The Zr-acetylide complex could not be isolated in any reaction, so the spectral data was obtained in situ.

Cp₂Zr(OMes)CCPh. ¹H NMR (500 MHz, PhBr-*d*₅) δ 7.53 (2H, m, *o*-ArH), 7.18 (3H, m, *p*-ArH & *m*-ArH(Ph)), 6.76 (2H, s, *m*-ArH(Mes)), 6.09 (10H, s, Cp), 2.21 (6H, s, *o*-Ar-CH₃), 2.19 (3H, s, *p*-Ar-CH₃) ppm.

1a + *PhCCD*. Mixture of products meant the Zr-acetylide complex could not be isolated. However colorless crystals of [D-NEt₃][B(C₆F₅)₄] formed in solution, which were filtered, washed with PhCl (3 \times 0.5 mL) and dried in vacuo. ¹⁵N-HMBC NMR (500 MHz, 51 MHz, PhBr-*d*₅) δ 452.2 (D-NEt₃) ppm. ¹H (400 MHz, CD₃CN) δ 3.22 (6H, q, D-N(CH₂CH₃)₃), 1.22 (9H, t, D-N(CH₂CH₃)₃) ppm. Deuteride signal not visible in ²H NMR spectrum due to solvent interactions. Nanospray (+ve detection) 103.1 *m/z* [D-NEt₃]⁺.

1b + *PhCCD*. Mixture of products meant the Zr-acetylide complex could not be isolated. However colorless crystals of [D-N(^{*i*}Pr)₂Et][B(C₆F₅)₄] formed in solution, which were filtered, washed with PhCl (3 \times 0.5 mL) and dried in vacuo. ¹⁵N-HMBC NMR (500 MHz, 51 MHz, PhBr-*d*₅) δ 424.8 (D-N(^{*i*}Pr)₂Et) ppm. ¹H (400 MHz, CD₃CN) δ 3.67 (2H, sept., N(CH(CH₃)₂)₂), 3.15 (2H, q, NCH₂CH₃), 1.38-1.25 (15H, m, N(CH(CH₃)₂)₂ and NCH₂CH₃) ppm. Deuteride signal not visible in ²H NMR spectrum due to solvent interactions. Nanospray (+ve detection) 131.2 *m/z* [D-N(^{*i*}Pr)₂Et]⁺.

1e + *PhCCD*. Mixture of products meant the Zr-acetylide complex could not be isolated. Spectral data shown for [D-NC₅H₃(CH₃)₂]⁺. ¹⁵N-HMBC NMR (500 MHz, 51 MHz, PhBr-*d*₅) δ 420.8 (D-

$\text{NC}_5\text{H}_3(\text{CH}_3)_2$ ppm. ^1H NMR (400 MHz, CD_3CN) δ 7.85 (1H, t, *p*-ArH), 7.27 (2H, dd, *m*-ArH), 2.55 (6H, s, -CH₃) ppm. ^2H NMR (77 MHz, $\text{PhBr-}d_5$) δ 12.45 (br, *D*- $\text{NC}_5\text{H}_3(\text{CH}_3)_2$) ppm. Nanospray (+ve detection) 109.1 *m/z* [*D*- $\text{NC}_5\text{H}_3(\text{CH}_3)_2$]⁺.

*Reactivity of [$\text{Cp}^*_2\text{ZrOMes}$][$\text{B}(\text{C}_6\text{F}_5)_4$] // LB (2a-e)*

In a glovebox, **2** (34.1 mg, 0.029 mmol) was dissolved in PhCl (0.5 mL) in an NMR tube fitted with a J. Youngs valve and C_6D_6 (one drop) was added as a reference in ^2H spectra. An equimolar amount of the Lewis base (**a** = NEt₃ (4.1 μL , 0.029 mmol), **b** = *i*Pr₂NEt (5.1 μL , 0.029 mmol), **c** = pyridine (2.4 μL , 0.029 mmol), **d** = 2-methylpyridine (2.9 μL , 0.029 mmol), **e** = 2,6-dimethylpyridine (3.4 μL , 0.029 mmol)) was then added. Excess phenylacetylene-*d* (3 drops) was then added. Samples **2a** and **2b** turned yellow within 5 min. **2c** did not demonstrate any reactivity. The Zr-acetylide complex could not be isolated in any reaction, so the spectral data was obtained in situ.

*Cp^*_2Zr(OMes)CCPh*. ^1H NMR (500 MHz, PhCl) δ 7.56 (2H, m, *o*-ArH), 6.69 (2H, s, *m*-ArH(Mes)), 2.16 (3H, s, *p*-Ar-CH₃), 1.88 (30H, s, Cp*), 1.79 (6H, s, *o*-Ar-CH₃) ppm. Remaining peaks were obscured by the PhCl solvent.

2a + *PhCCD*. Mixture of products meant the Zr-acetylide complex could not be isolated. However colorless crystals of [*D*-NEt₃][$\text{B}(\text{C}_6\text{F}_5)_4$] formed in solution, which were filtered, washed with PhCl (3 \times 0.5 mL) and dried in vacuo. ^{15}N -HMBC NMR (500 MHz, 51 MHz, PhCl/ C_6D_6) δ 439.7 (*D*-NEt₃) ppm. ^1H (400 MHz, $\text{CH}_3\text{CN}/\text{C}_6\text{D}_6$) δ 3.06 (6H, q, *D*-N(CH₂CH₃)₃), 1.22 (9H, t, *D*-N(CH₂CH₃)₃) ppm. Deuteride signal not visible in ^2H NMR spectrum due to solvent interactions. Nanospray (+ve detection) 103.1 *m/z* [*D*-NEt₃]⁺.

2b + *PhCCD*. Mixture of products meant the Zr-acetylide complex could not be isolated. However colorless crystals of [*D*-N(*i*Pr)₂Et][$\text{B}(\text{C}_6\text{F}_5)_4$] formed in solution, which were filtered,

washed with PhCl (3 × 0.5 mL) and dried in vacuo. ¹⁵N-HMBC NMR (500 MHz, 51 MHz, PhCl/C₆D₆) signal not seen (see Results and Discussion). ¹H (400 MHz, CH₃CN/C₆D₆) δ 3.59 (2H, sept., N(CH(CH₃)₂)₂), 3.07 (2H, q, NCH₂CH₃), 1.33-1.25 (15H, m, N(CH(CH₃)₂)₂ and NCH₂CH₃) ppm. Deuteride signal not visible in ²H NMR spectrum due to solvent interactions. Nanospray (+ve detection) 131.2 *m/z* [D-N(^{*i*}Pr)₂Et]⁺.

2d + *PhCCD*. Mixture of products meant the Zr-acetylide complex could not be isolated. Spectral data shown for [D-NC₅H₄(CH₃)]⁺. ¹⁵N-HMBC NMR (500 MHz, 51 MHz, PhCl/C₆D₆) δ 426.5 (D-NC₅H₄(CH₃)) ppm. ¹H NMR (400 MHz, PhCl/C₆D₆) δ 2.05 (3H, s, -CH₃) ppm, aromatic peaks obscured. ²H NMR (77 MHz, PhCl/C₆D₆) δ 12.38 (br, D-NC₅H₄(CH₃)) ppm. Nanospray (+ve detection) 95.1 *m/z* [D-NC₅H₄(CH₃)]⁺.

2e + *PhCCD*. Mixture of products meant the Zr-acetylide complex could not be isolated. Spectral data shown for [D-NC₅H₃(CH₃)₂]⁺. ¹⁵N-HMBC NMR (500 MHz, 51 MHz, PhCl/C₆D₆) δ 421.6 (D-NC₅H₃(CH₃)₂) ppm. ¹H NMR (400 MHz, CD₃CN) δ 7.85 (1H, t, *p*-ArH), 7.27 (2H, *dd*, *m*-ArH), 2.55 (6H, s, -CH₃) ppm. ²H NMR (77 MHz, CD₃CN) δ 12.47 (br, D-NC₅H₃(CH₃)₂) ppm. Nanospray (+ve detection) 109.1 *m/z* [D-NC₅H₃(CH₃)₂]⁺.

Catalytic Dehydrocoupling of Me₂NH·BH₃

Reactivity of [Cp₂ZrOMes][B(C₆F₅)₄] // LB (**1a-e**)

In a glovebox, **1** (18.7 mg, 0.018 mmol) and Me₂NH·BH₃ (10.6 mg, 0.18 mmol) were weighed into separate vials and dissolved in PhBr-*d*₅ (0.5 mL). The relevant Lewis base (**a** = NEt₃ (2.5 μL, 0.018 mmol), **b** = ^{*i*}Pr₂NEt (3.2 μL, 0.018 mmol), **c** = pyridine (1.5 μL, 0.018 mmol), **d** = 2-methylpyridine (1.8 μL, 0.018 mmol), **e** = 2,6-dimethylpyridine (2.1 μL, 0.018 mmol)) was then added to **1**. The two solutions were then combined, and the fully mixed solution was transferred to a quartz J. Youngs NMR tube before the relevant spectra were then collected. No reaction was

seen for **1c**, however the relevant spectra for the reactions of **1a**, **1b**, **1d**, and **1e** can be found in the Supporting Information (Figures S16-S20).

*Reactivity of $[\text{Cp}^*_2\text{ZrOMes}][\text{B}(\text{C}_6\text{F}_5)_4]$ // LB (**2a-e**)*

In a glovebox, **2** (21.2 mg, 0.018 mmol) and $\text{Me}_2\text{NH}\cdot\text{BH}_3$ (10.6 mg, 0.18 mmol) were weighed into separate vials and dissolved in $\text{PhBr-}d_5$ (0.5 mL). The relevant Lewis base (**a** = NEt_3 (2.5 μL , 0.018 mmol), **b** = $i\text{Pr}_2\text{NEt}$ (3.2 μL , 0.018 mmol), **c** = pyridine (1.5 μL , 0.018 mmol), **d** = 2-methylpyridine (1.8 μL , 0.018 mmol), **e** = 2,6-dimethylpyridine (2.1 μL , 0.018 mmol)) was then added to **2**. The two solutions were then combined, and the fully mixed solution was transferred to a quartz J. Youngs NMR tube before the relevant spectra were then collected (please see Supporting Information, Figures S21-S25).

Catalytic Dehydrocoupling of $\text{Me}_2\text{NH}\cdot\text{BH}_3$ at 60 °C

The reactions were prepared for **1a**, **1e**, and **2e** using the same method shown above, with the spectra then collected in an NMR spectrometer set to 60 °C. Please see the Supporting Information for the collected spectra (Figures S26-S31).

ASSOCIATED CONTENT

Supporting Information DOSY spectra for **1a-e** and **2a-e**, experimental procedures and analytical data (^{11}B NMR spectra and reaction profiles) for all catalytic reactions, crystallographic data for **2c** and **2d** (PDF), crystallographic data (CIF)

AUTHOR INFORMATION

Corresponding Author

*wass.d@cardiff.ac.uk

Notes

The authors declare no competing financial interest.

Acknowledgements

H.B.H. would like to acknowledge Dr. Paul Gates and the University of Bristol Mass Spectrometry Service for their assistance.

References

1. Welch, G. C.; San Juan, R. R.; Masuda, J. D.; Stephan, D. W., Reversible, Metal-Free Hydrogen Activation. *Science* **2006**, *314*, 1124-1126.
2. Stephan, D. W.; Erker, G., Frustrated Lewis Pair Chemistry: Development and Perspectives. *Angew. Chem. Int. Ed.* **2015**, *54*, 6400-6441.
3. Stephan, D. W.; Erker, G., Frustrated Lewis Pairs: Metal-free Hydrogen Activation and More. *Angew. Chem. Int. Ed.* **2010**, *49*, 46-76.
4. Chapman, A. M.; Haddow, M. F.; Wass, D. F., Frustrated lewis pairs beyond the main group: synthesis, reactivity, and small molecule activation with cationic zirconocene-phosphinoaryloxide complexes. *J. Am. Chem. Soc.* **2011**, *133*, 18463-18478.
5. Chapman, A. M.; Haddow, M. F.; Wass, D. F., Cationic Group 4 Metallocene-(o-Phosphanylaryl)oxido Complexes: Synthetic Routes to Transition-Metal Frustrated Lewis Pairs. *Eur. J. Inorg. Chem.* **2012**, *2012*, 1546-1554.
6. Xu, X.; Kehr, G.; Daniliuc, C. G.; Erker, G., 1,1-Carbozirconation: Unusual Reaction of an Alkyne with a Methyl Zirconocene Cation and Subsequent Frustrated Lewis Pair Like Reactivity. *Angew. Chem. Int. Ed.* **2013**, *52*, 13629-13632.

7. Xu, X.; Kehr, G.; Daniliuc, C. G.; Erker, G., Reactions of a Cationic Geminal Zr⁺/P Pair with Small Molecules. *J. Am. Chem. Soc.* **2013**, *135*, 6465-6476.
8. Xu, X.; Kehr, G.; Daniliuc, C. G.; Erker, G., Formation of unsaturated vicinal Zr⁺/P frustrated Lewis pairs by the unique 1,1-carbozirconation reactions. *J. Am. Chem. Soc.* **2014**, *136*, 12431-12443.
9. Xu, X.; Kehr, G.; Daniliuc, C. G.; Erker, G., Stoichiometric Reactions and Catalytic Hydrogenation with a Reactive Intramolecular Zr⁺/Amine Frustrated Lewis Pair. *J. Am. Chem. Soc.* **2015**, *137*, 4550-4557.
10. Normand, A. T.; Daniliuc, C. G.; Wibbeling, B.; Kehr, G.; Le Gendre, P.; Erker, G., Phosphido- and Amidozirconocene Cation-Based Frustrated Lewis Pair Chemistry. *J. Am. Chem. Soc.* **2015**, *137*, 10796-10808.
11. Jian, Z.; Daniliuc, C. G.; Kehr, G.; Erker, G., Frustrated Lewis Pair vs Metal–Carbon σ -Bond Insertion Chemistry at an o-Phenylene-Bridged Cp₂Zr⁺/PPh₂ System. *Organometallics* **2017**, *36*, 424-434.
12. Neu, R. C.; Otten, E.; Lough, A.; Stephan, D. W., The synthesis and exchange chemistry of frustrated Lewis pair-nitrous oxide complexes. *Chemical Science* **2011**, *2*, 170-176.
13. Metters, O. J.; Forrest, S. J. K.; Sparkes, H. A.; Manners, I.; Wass, D. F., Small Molecule Activation by Intermolecular Zr(IV)-Phosphine Frustrated Lewis Pairs. *J. Am. Chem. Soc.* **2016**, *138*, 1994-2003.

14. Metters, O. J.; Flynn, S. R.; Dowds, C. K.; Sparkes, H. A.; Manners, I.; Wass, D. F., Catalytic Dehydrocoupling of Amine–Boranes using Cationic Zirconium(IV)–Phosphine Frustrated Lewis Pairs. *ACS Catal.* **2016**, *6*, 6601-6611.
15. Clark, E. R.; Ingleson, M. J., N-Methylacridinium Salts: Carbon Lewis Acids in Frustrated Lewis Pairs for σ -Bond Activation and Catalytic Reductions. *Angew. Chem. Int. Ed.* **2014**, *53*, 11306-11309.
16. Chernichenko, K.; Nieger, M.; Leskela, M.; Repo, T., Hydrogen activation by 2-boryl-N,N-dialkylanilines: a revision of Piers' ansa-aminoborane. *Dalton Trans.* **2012**, *41*, 9029-9032.
17. Chernichenko, K.; Kótai, B.; Pápai, I.; Zhivonitko, V.; Nieger, M.; Leskelä, M.; Repo, T., Intramolecular Frustrated Lewis Pair with the Smallest Boryl Site: Reversible H₂ Addition and Kinetic Analysis. *Angew. Chem. Int. Ed.* **2015**, *54*, 1749-1753.
18. Chernichenko, K.; Lindqvist, M.; Kótai, B.; Nieger, M.; Sorochkina, K.; Pápai, I.; Repo, T., Metal-Free sp²-C–H Borylation as a Common Reactivity Pattern of Frustrated 2-Aminophenylboranes. *Journal of the American Chemical Society* **2016**, *138*, 4860-4868.
19. Binding, S. C.; Zaher, H.; Mark Chadwick, F.; O'Hare, D., Heterolytic activation of hydrogen using frustrated Lewis pairs containing tris(2,2[prime or minute],2[prime or minute][prime or minute]-perfluorobiphenyl)borane. *Dalton Trans.* **2012**, *41*, 9061-9066.
20. Courtemanche, M.-A.; Rochette, E.; Legare, M.-A.; Bi, W.; Fontaine, F.-G., Reversible hydrogen activation by a bulky haloborane based FLP system. *Dalton Transactions* **2016**, *45*, 6129-6135.

21. Iashin, V.; Chernichenko, K.; Pápai, I.; Repo, T., Atom-Efficient Synthesis of Alkynylfluoroborates Using BF₃-Based Frustrated Lewis Pairs. *Angew. Chem. Int. Ed.* **2016**, *55*, 14146-14150.
22. Korte, L. A.; Blomeyer, S.; Heidemeyer, S.; Nissen, J. H.; Mix, A.; Neumann, B.; Stammler, H.-G.; Mitzel, N. W., Intramolecular Lewis pairs with two acid sites - reactivity differences between P- and N-based systems. *Dalton Trans.* **2016**, *45*, 17319-17328.
23. Li, H.; Wen, M.; Lu, G.; Wang, Z.-X., Catalytic metal-free intramolecular hydroaminations of non-activated aminoalkenes: A computational exploration. *Dalton Trans.* **2012**, *41*, 9091-9100.
24. Liu, L.; Vankova, N.; Heine, T., A kinetic study on the reduction of CO₂ by frustrated Lewis pairs: from understanding to rational design. *Phys. Chem. Chem. Phys.* **2016**, *18*, 3567-3574.
25. Maier, A. F. G.; Tussing, S.; Schneider, T.; Flörke, U.; Qu, Z.-W.; Grimme, S.; Paradies, J., Frustrated Lewis Pair Catalyzed Dehydrogenative Oxidation of Indolines and Other Heterocycles. *Angew. Chem. Int. Ed.* **2016**, *55*, 12219-12223.
26. Theuergarten, E.; Schlosser, J.; Schluns, D.; Freytag, M.; Daniliuc, C. G.; Jones, P. G.; Tamm, M., Fixation of carbon dioxide and related small molecules by a bifunctional frustrated pyrazolylborane Lewis pair. *Dalton Trans.* **2012**, *41*, 9101-9110.
27. von Wolff, N.; Lefèvre, G.; Berthet, J. C.; Thuéry, P.; Cantat, T., Implications of CO₂ Activation by Frustrated Lewis Pairs in the Catalytic Hydroboration of CO₂: A View Using N/Si+ Frustrated Lewis Pairs. *ACS Catal.* **2016**, *6*, 4526-4535.

28. Yepes, D.; Jaque, P.; Fernández, I., Deeper Insight into the Factors Controlling H₂ Activation by Geminal Aminoborane-Based Frustrated Lewis Pairs. *Chem. - Eur. J.* **2016**, *22*, 18801-18809.
29. Yepes, D.; Jaque, P.; Fernández, I., Hydrogenation of Multiple Bonds by Geminal Aminoborane-Based Frustrated Lewis Pairs. *Chem. - Eur. J.* **2018**, *24*, 8833-8840.
30. Zhang, Y.; Miyake, G. M.; John, M. G.; Falivene, L.; Caporaso, L.; Cavallo, L.; Chen, E. Y. X., Lewis pair polymerization by classical and frustrated Lewis pairs: acid, base and monomer scope and polymerization mechanism. *Dalton Trans.* **2012**, *41*, 9119-9134.
31. Flynn, S. R.; Metters, O. J.; Manners, I.; Wass, D. F., Zirconium-Catalyzed Imine Hydrogenation via a Frustrated Lewis Pair Mechanism. *Organometallics* **2016**, *35*, 847-850.
32. Linnell, R., Notes- Dissociation Constants of 2-Substituted Pyridines. *J. Org. Chem.* **1960**, *25*, 290-290.
33. Fujii, T.; Nishida, H.; Abiru, Y.; Yamamoto, M.; Kise, M., Studies on Synthesis of the Antibacterial Agent NM441. II. Selection of a Suitable Base for Alkylation of 1-Substituted Piperazine with 4-(Bromomethyl)-5-methyl-1, 3-dioxol-2-one. *Chem. Pharm. Bull.* **1995**, *43*, 1872-1877.
34. Matos, J. M. E.; Lima-Neto, B. S., Acyclic amines as ancillary ligands in Ru-based catalysts for ring-opening metathesis polymerization: Probing the electronic and steric aspects of cyclic and acyclic amines. *J. Mol. Catal. A: Chem.* **2006**, *259*, 286-291.
35. Clarke, K.; Rothwell, K., 377. A kinetic study of the effect of substituents on the rate of formation of alkylpyridinium halides in nitromethane solution. *J. Chem. Soc.* **1960**, *0*, 1885-1895.

36. Rosorius, C.; Kehr, G.; Fröhlich, R.; Grimme, S.; Erker, G., Electronic Control of Frustrated Lewis Pair Behavior: Chemistry of a Geminal Alkylidene-Bridged Per-pentafluorophenylated P/B Pair. *Organometallics* **2011**, *30*, 4211-4219.
37. Liedtke, R.; Fröhlich, R.; Kehr, G.; Erker, G., Frustrated Lewis Pair Reactions With Bis-Acetylenic Substrates: Exploring the Narrow Gap Separating Very Different Competing Reaction Pathways. *Organometallics* **2011**, *30*, 5222-5232.
38. Rosorius, C.; Daniliuc, C. G.; Fröhlich, R.; Kehr, G.; Erker, G., Structural features and reactions of a geminal frustrated phosphane/borane Lewis pair. *J. Organomet. Chem.* **2013**, *744*, 149-155.
39. Rosorius, C.; Möricke, J.; Wibbeling, B.; McQuilken, A. C.; Warren, T. H.; Daniliuc, C. G.; Kehr, G.; Erker, G., Frustrated Lewis Pair Chemistry Derived from Bulky Allenyl and Propargyl Phosphanes. *Chem. - Eur. J.* **2016**, *22*, 1103-1113.
40. Elmer, L.-M.; Kehr, G.; Daniliuc, C. G.; Siedow, M.; Eckert, H.; Tesch, M.; Studer, A.; Williams, K.; Warren, T. H.; Erker, G., The Chemistry of a Non-Interacting Vicinal Frustrated Phosphane/Borane Lewis Pair. *Chem. - Eur. J.* **2017**, *23*, 6056-6068.
41. Bush, R. C.; Angelici, R. J., Phosphine basicities as determined by enthalpies of protonation. *Inorg. Chem.* **1988**, *27*, 681-686.
42. Chapman, A. M.; Haddow, M. F.; Wass, D. F., Frustrated Lewis Pairs beyond the Main Group: Cationic Zirconocene-Phosphino-aryloxide Complexes and Their Application in Catalytic Dehydrogenation of Amine Boranes. *J. Am. Chem. Soc.* **2011**, *133*, 8826-8829.

SYNOPSIS A series of intermolecular frustrated Lewis pairs (FLPs), formed from the combination of a zirconocene with an amine or pyridine Lewis base, are reported and used for the activation of a series of small molecules including CO₂, D₂, THF, and PhCCD. In addition to this, the catalytic dehydrocoupling of Me₂NH·BH₃ is also reported, allowing comparisons with previously reported Zr/P intermolecular FLPs.

